- 1 Phytonanoremediation by Avicennia Germinans (black mangrove) and Nano Zero
- 2 Valent Iron for Heavy Metal Uptake from Cienaga Las Cucharillas Wetland Soils
- 3 Keyla T. Soto Hidalgo^{1*}, Pedro J. Carrión-Huertas², Richard T. Kinch³, Luis E.
- 4 Betancourt⁴, and Carlos R. Cabrera^{3*}
- ¹University High School, University of Puerto Rico, Río Piedras Campus, San Juan,
- 6 Puerto Rico 00931
- ²Corredor del Yaguazo Inc, Ciénaga Las Cucharillas, Cataño, Puerto Rico, 00962
- 8 ³Department of Chemistry, 17 Ave. Universidad STE 1701, University of Puerto Rico,
- 9 Río Piedras Campus, San Juan, Puerto Rico 00925-2537
- ⁴ Chemistry Department, Brookhaven National Laboratory, Upton, NY 11973
- 12 Abstract

13 Plants may be used to remove or convert pollutants into harmless products by 14 bioaccumulating, degrading, extracting, or immobilizing them. Phytoremediation 15 processes offer advantages over traditional remediation methods such as chemical 16 oxidation, excavation, and thermal treatments. A combined usage of mangroves and 17 nano zero valent iron (nZVI), could be implemented for the remediation of Cadmium 18 (Cd), Lead (Pb) and Arsenic (As) in contaminated wetlands. Here, 19 phytonanoremediation process which combined A. germinans and nZVI was evaluated 20 for a period of 5 months using contaminated soil from Cienaga las Cucharillas, Cataño, 21 Puerto Rico. We evaluate the efficiency of the phytonanoremediation process using 15 22 individuals of A. germinans with and without nZVI to remove Cd, Pb and As in 23 contaminated soil by inductively coupled plasma (ICP) analysis measurements. A plant 24 tissue analysis of root, stem and leave of A. germinans after nZVI exposure in their 25 corresponding soil was conducted using X-ray photoelectron spectroscopy (XPS) and 26 transmission electron microscopy (TEM) techniques. Bioaccumulation factors (BAF) and 27 Translocation factors (TF) were calculated. A BAF < 1 combined with a TF < 1 indicates

- 28 that *A. germinans* is not working as a hyperaccumulator plant, but rather as excluders for
- 29 Cd and Pb metals. Data obtained in the nanoenvironmental project suggested that the
- interaction of nZVI with *A. germinans* is an efficient way to enhance the bioavailability of
- 31 Pb²⁺ and Cd²⁺ and enable plants to better translocate them into their aerial parts.
- 32 *To whom correspondence should be addressed: keyla.soto@upr.edu and
- 33 <u>carlos.cabrera2@upr.edu</u>
- 34 Keywords: remediation, wetland, nZVI, heavy metals, Puerto Rico

Introduction

The presence of heavy metals in soil or water is one of the common stresses that limit plant growth and development (Liphadzi and Kirkham, 2006). Many studies have shown that plant species, which grow in polluted environments, may be stressed in various ways (Azzazy M. F. 2020; Blande et al., 2014). For example, bioaccumulation of metals to toxic concentrations (through direct uptake by the roots, stems, or shoots) results in malfunctioning of their physiological systems (Dahmani-Muller et al., 2000; Plekhanov and Chemeris, 2003). Plants have developed several strategies to resist the toxicity of heavy metals, including active efflux, sequestration, and binding of heavy metals inside the cells by strong ligands (Hall, 2002).

Several studies have developed strategies involving the use of plants to remove contaminants from water and soil. Interestingly, plants that are able to decontaminate soils do one or more of the following: (1) plant uptake of the contaminant from the soil into their roots; (2) bind the contaminant into their root tissue by a physical or chemical process; or (3) transport the contaminant from their roots into growing shoots and prevent or inhibit the contaminant from leaching out of the soil (Tangahu et al., 2011). In decontamination processes using plants, it is preferable to have the metal accumulated in the shoots as opposed to the roots. The metal in the shoot can be cut from the plant and removed (Raskin and Ensley, 2000). If the metals are concentrated in the roots, the entire plant needs to be removed. This would not only increase the costs of phytoremediation,

due to the need for additional labor and plantings, but also increase the time it takes for the new plants to establish themselves in the environment and begin accumulation of metals (Kamnev and van der Lelie, 2000). In addition, the availability of metals in the soil for plant uptake is another limitation for successful phytoremediation (Raskin and Ensley, 2000).

In environmental remediation, nano zero valent iron (nZVI) has been used successfully (Bae et al., 2018; Bolade et al., 2020; Garg et al., 2018; Kim et al., 2018; Kocur et al., 2014; Zou et al., 2016). For example, nZVI has been injected into contaminated sandy subsurface areas in Sarnia, Ontario, (Kocur et al., 2014) and coupled with functional anaerobic bacteria for groundwater remediation. However, many studies that proposed the use of nZVI for environmental decontamination have focused mainly on the advantages, and very few in the mechanisms of phytotoxicity, uptake, translocation, and bioaccumulation in organisms including plants and animals present in the ecosystem (Paz-Alberto and Sigua, 2013; Zhang et al., 2015).

The research objectives are: (1) building a nanoremediation system to evaluate the interaction of nZVI and *A. germinans* in contaminated soil with Cd²⁺, Pb²⁺ and As²⁺ from Ciénaga las Cucharillas, (2) evaluate the efficiency of the phytonanoremediation process using *A. germinans* with and without nZVI to remove Cd, Pb and As in contaminated soil by inductively coupled plasma (ICP) analysis measurements, and (3) analyze the plant tissue of *A. germinans* after nZVI exposure using X-ray photoelectron spectroscopy (XPS) and transmission electron microscopy (TEM) techniques.

Materials and Methods Section

78 Study area

The Cienaga las Cucharillas located at Cataño, Puerto Rico have an extension of approximately 500 ha, which is composed primarily of herbaceous wetlands, mangroves, and open water areas (see Fig. 1). This wetland is an extensive saltwater and freshwater

area in the northwestern corner of the San Juan Bay. This wetland receives industrial runoff from several industrial parks and raw sewage discharges form the surrounding communities (i.e. Juana Matos and Puente Blanco).

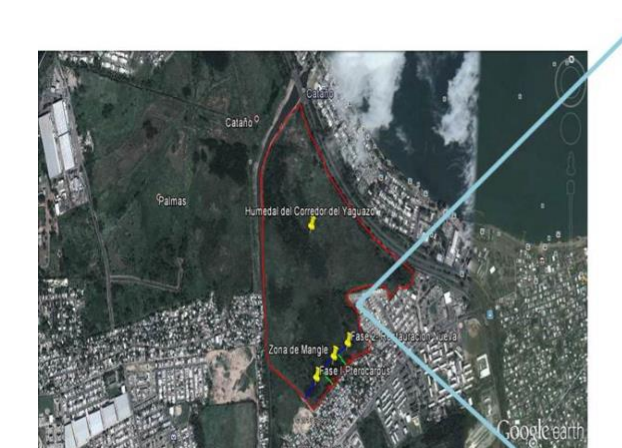




Figure 1. Localization of Cienaga Las Cucharillas in Cataño, Puerto Rico identified as Y1 to Y9 sampling zone.

The sampling zone of wetland was divided into 9 plots under different land use types (Pterocarpus zone, mangroves zone, and a new zone of restoration) identified as Y1 to Y9 (three plots for each zone) as shown in Figure 1. The wetland soils were collected at a depth of 10 cm. Soil samples were placed in polyethylene bags and returned to the laboratory. The soil analyses were performed using Inductively Coupled Plasma (ICP) to determine the sites with high concentrations of Cd, As and Pb. ICP-AES is an optical emission spectrometry where an aerosol sample is placed in a plasma source of 8000K, is broken down, and its component atoms are excited. When the excited atoms return to low energy states, they emit electromagnetic radiation. The element type is determined based on the emitted wavelength, and their wavelength intensities are directly proportional to the concentration of each species.

Acclimation of A. germinans

The seedlings of *A. germinans* were obtained from Cienaga las Cucharillas, through direct harvesting during the month of July 2015. Mangrove plants were first kept in a nursery station under shaded cover using the same substrate of Cienaga las Cucharillas to maintain their natural conditions. The growth and maintenance of these plants once brought from the wetland was performed in a greenhouse located in The Botanical Garden of the University of Puerto Rico, Rio Piedras Campus, San Juan.

After an acclimation period of 28 to 30 days, surviving plants were considered fully adapted to their new environmental conditions in the constructed nanoremediation system as seen in Fig. 2. The height of each plant was measured from the bottom of the stem to the tip of the last leaf for a period of five months. The concentration chlorophyll was measured as an important indicator of plant health using a Chlorophyll meter model SPAD (Konica Minolta company) on each plant for a period of five months. The chlorophyll meter measured the light transmittance in two wavelength ranges (600 to 700 and 400 to 500 nm) to determine the relative amount of chlorophyll in the leaves because

Preparation of nZVI

In the present work, nZVI were tested for their ability to reduce and remove Pb, As, and Cd in a phytonanoremediation process. The nZVI particles were prepared by the reduction of an aqueous iron salt solution using an easily controlled and effective reductant: sodium borohydride (NaBH₄) (Soto-Hidalgo et al., 2015). A 0.6 M solution of FeCl₃·6H₂O was prepared in 30 mL of ethanol (87% v/v). The solution was purged with N₂ for 30 minutes to remove oxygen prior to the reaction to prevent the rapid oxidation of the metallic iron product. The solution was titrated by adding a total of 100 mL of a 0.8M NaBH₄ solution under nitrogen. After 30 minutes of stirring with a magnetic bar at 700 rpm, the solution was filtered using a 0.22µm filter paper (Millipore) under vacuum

of its selective absorption of a specific wavelength of light.

suction at 25 °C. Finally, the sample was rinsed three times with 99% absolute ethanol and the resulting filtered samples were placed immediately in a vacuum desiccator.

Phytonanoremediation System

The nanoremediation system shown in Fig. 2 was constructed using a design of direct injection in soil. All the chambers in the system had soil from contaminated zone of the Cienaga las Cucharillas with the highest Cd, As, and Pb concentrations. The soil samples were each characterized and analyzed by ICP-AES before introducing them into system.

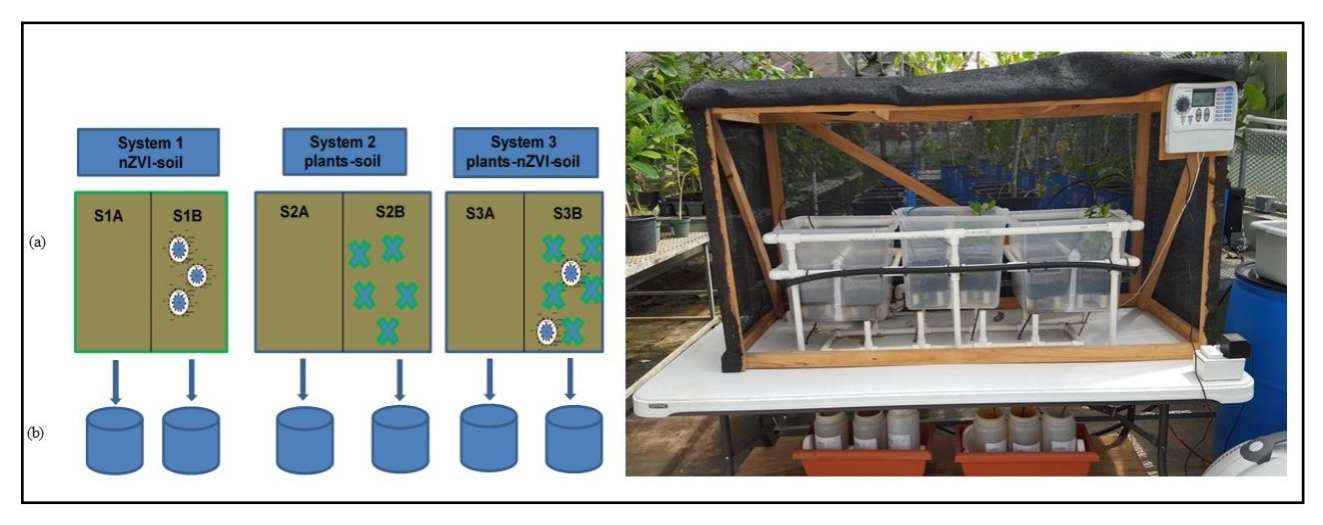


Figure 2. Schematic (left) and image (right) of the nanoremediation system's two major components: a) chambers that contain nZVI and wetland soil; plants/wetland soil; and plants/nZVI/wetland soil, respectively (b) HDPE bottles for each sample to store and collect water from the soil. Soils S1A, S2A, and S3A are control samples. S1B and S2B contain nZVI and A. germinans, respectively. Soil S3B contains both nZVI and A. germinans. In the figure, **x** represent de A. germinans and the circle represent the system with the nZVI.

The system is divided into three sets of two chambers: S1A-S1B, S2A-S2B, and S3A-S3B. Each set has a control chamber and an experimental chamber to assure the precision and accuracy of the data. Six portable caddies of $14.3 \text{ cm} \times 28.6 \text{ cm} \times 12.7 \text{ cm}$

were used to place each sample of 500 grams of soil. These caddies were fixed inside of chambers of 16.5 cm to collect water. Each chamber was separated using 17.7 cm cylindrical PVC pipes of 3.8 cm of internal diameter. Each system was connected individually to a high-density polyethylene (HDPE) bottle to collect the soil filtrated water. The water system was connected to each chamber independently at a flowrate of 500mL/min, seven days per week and was flowed once per day for 2 minutes. This study was done for a period of five months under greenhouse conditions.

The SA systems included soil as control (S1A, S2A, and S3A). The S1B system contained only wetland soil with 3 g/L of nZVI injected at 6 points. This injection was done once using a plastic pipette. In the S2B system, 15 individual *A.germinans* seedlings were transplanted to analyze the ability of this species to remove the Cd, As, and Pb metals from the soil. Comparing systems S1B and S2B was the cornerstone for this research, since it would essentially determine the efficiency of *A. germinans* and nZVI individually to remove these heavy metals. Following the protocol used for S1B, nZVI were injected in soil of the system S3B, where another 15 *A. germinans* seedlings were transplanted. This later system was evaluated as a phytonanoremediation process to compare the collective efficiency of these two processes in removing Cd, As, and Pb from soil. A Bioaccumulator Factor (BAF) technique was used to evaluate quantitatively the accumulation of target pollutants in the biomass. It is typically defined as:

$$BAF = C_{\text{shoot}}/C_{\text{soil}} \tag{4}$$

C_{shoot} and C_{soil} are metals concentration in the plant shoot (mg·kg⁻¹) and soil (mg·kg⁻¹), respectively (MacFarlane and Burchett, 2002). BAF was the metric chosen to categorize these plants as: 1) hyperaccumulators; 2) accumulators, which accumulate metals over 1 mg·kg⁻¹, or 3) excluders, which accumulate metals under 1 mg·kg⁻¹ to those samples. Complimentary to the BAF analysis, another technique was used to measure the Cd, Pb, and As translocation from shoot to root which is given below:

$$TF = C_{\text{shoot}}/C_{\text{root}}, \tag{5}$$

where C_{shoot} and C_{root} are metals concentration in the shoot (mg·kg⁻¹) and root of plant (mg·kg⁻¹), respectively (Peters et al., 1997). A Translocation factor (TF) value larger than 1 represents the effective translocation of metals to the shoot from the root. For this study, 500 grams of contaminated soil was used. A 3g/L injection of nZVI was made into the soil to the experimental systems. The ratio of mass of Fe to volume of soil was 0.004 (Wang et al., 2016).

Metal analysis in Tissue, Soil and Water

To determine the effect of the nanoparticles in the amount of Cd, Pb, and As ions on each system of soil, water and plants after treatment period time, all the samples were processed and analyzed using ICP-AES Model Perkin Elmer 4300 DV with a detection limit of 0.002 ppm. The method used for each digestion is EPA 6010 B, this includes analysis of the three metals in water, soil and plant tissue. Removal efficiency (%) was determined for Cd, Pb and As in each experimental system. The removal efficiency of metals was defined as follows:

Removal efficiency (%) =
$$\frac{C_0 - C_t}{C_0} \times 100$$
 (6)

 C_0 is defined as the initial concentration of metals (mg/kg) and C_t as the concentration of metals (mg/kg) at reaction time (t).

The three different sections of the *A. germinans* plants: roots, stem, and leaves were analyzed by X-ray photoelectron spectroscopy (XPS). The samples were evaluated to detect the presence of nZVI in *A. germinans*. Fig. 3 shows the XPS instrument and sample preparation. XPS analyzes the outer 5 nm of the surface, as such is very sensitive to varying chemical forms of elements on the surface. The purpose of these studies was to characterize the differences between *A. germinans* plants in control and treated systems.

In the S3B system, the plants interacted with nZVI (3g/L) for a period of 5 months. These samples were root, leaf, or stem tips (0.5 cm). The cut sections were carefully placed and manipulated on conducting tape by holding the end by forceps. This analysis was performed to track the mobility of nZVI in various parts of *A. germinans*. Plants represent a complex problem for analysis, particularly the root surface interface. The leaves, stem, and roots were thinly cut into transversal portions for the XPS analysis. XPS binding energy spectra were obtained using a PHI spectrometer equipped with an Al K α mono and polychromatic x-ray source operating at 15 kV, 350 W and pass energy of 58.70 eV. All the binding energies reported were corrected fixing the carbon 1s peak (C 1s) at 284.5 eV. A transmission electron microscope, Thermo-Fisher FEI GF20, equipped with a Monochromated Oxford Aztec X-ray detector was used to examine the plant morphology.

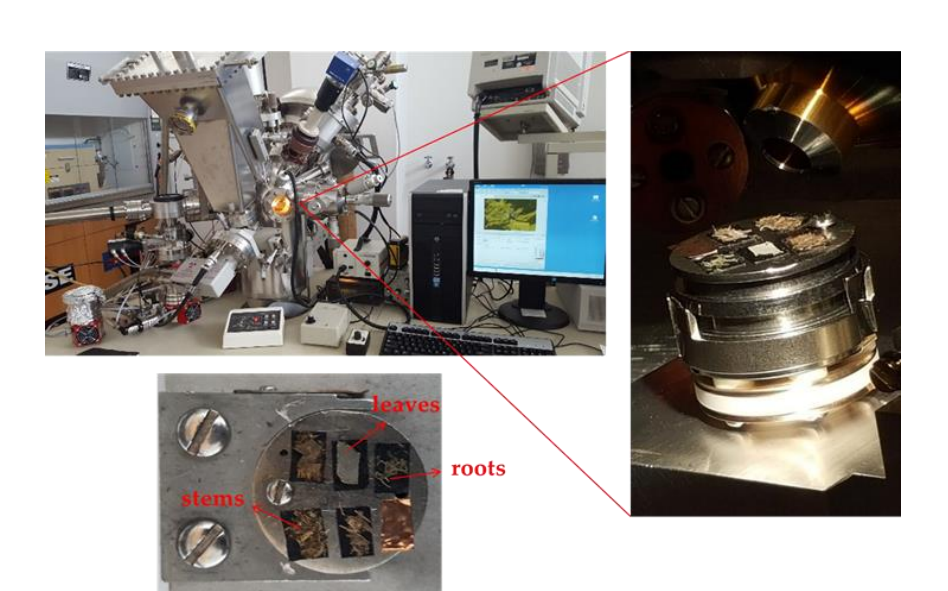


Figure 3. Preparation of samples in holder X-ray photoelectron spectroscopy analysis that include leaves, stem, and root of *A. germinans* of system S2B and S3B.

Chlorophyll analysis in A. germinans

Chlorophyll content changes when a plant is stressed. An SPAD meter can be used

for a rapid determination of the chlorophyll content of the individual leaves (Percival et al., 2008). Chlorophyll analyses were measured in *A. germinans* in S2B and S3B system to compare the possible effect of nZVI in plants. When *A. germinans* plants were at the same growth stages in the system S2B and S3B, SPAD chlorophyll meter readings were taken monthly in 5 to 10 leaves of each plant.

Results and discussions

The average concentration of Cd, Pb and As for each soil sample in the nanoremediation system after 5 months of treatment determined by (ICP-AES) analysis are shown in Fig. 4. The initial concentration of As for all the systems except S1B was 29.5 mg/kg. The system S1B had an initial concentration of 25.5 mg/kg. The precise measurement of these initial concentrations was essential at the beginning of the experiments because the soil matrix in the wetland is not homogeneous.

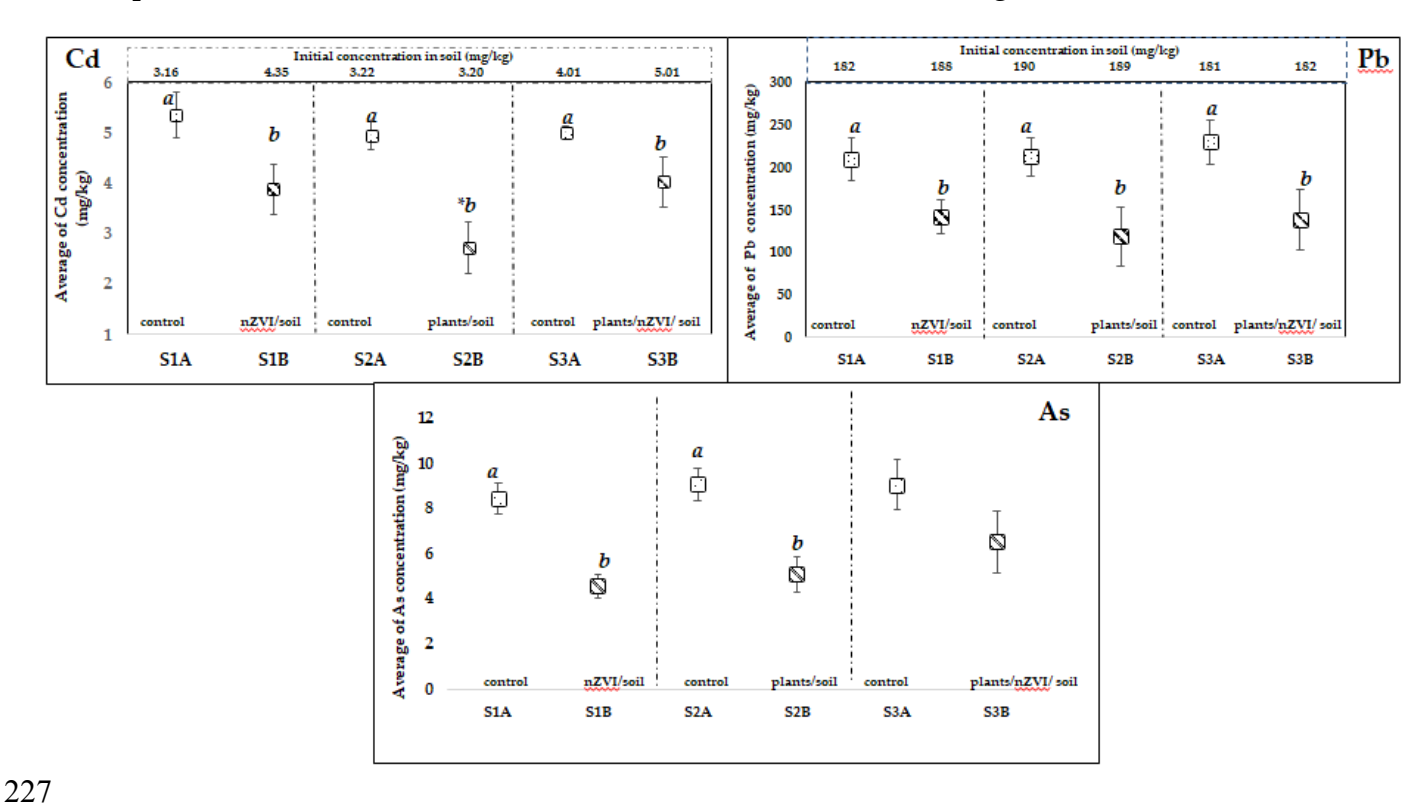


Figure 4. Average concentration of As, Cd, and Pd metals in control and treated soils for a period of 5 months (mean \pm SD). The values at the top of each graph are the initial

concentrations for each of the soil systems (S1A to S3B). Mean values not sharing a common letter (a or b) differ **significantly** according to Tukey's test (P<0.05). Symbols represent the significant difference between treatments

Figure 4 shows the ICP-AES analysis of the average concentration of Cd, Pb and As in all the systems. Each system was analyzed weekly for each metal in a period of 5 months. The results of Tukey's test show that system S2B decreased the Cd concentration more than in the other systems, probably due to the bioavailable form of Cd present in soil. For the control systems (SA), the slight increase of Cd and Pb concentration is probably due to the input of this metal concentration permissible in drinking water over the 5 months of the experiment (see Figs. S1 and S2). Results for Pb concentration show that treatment systems had a decrease in concentration at the end of the experiment.

Tissue analysis of A. germinans plants

Average values of SPAD and height measures are shown in Fig. 5. The SPAD chlorophyll meter appeared to be a useful tool for *A. germinans*. Results indicate that the concentration of chlorophyll content of these systems were relatively close. Furthermore, there was not a significant difference between of *A. germinans* in the treated groups and the control group at the end of experiment for both parameters. These results confirm that nZVI can interact with *A. germinans* to remove heavy metals without noticeably affecting its physiology.

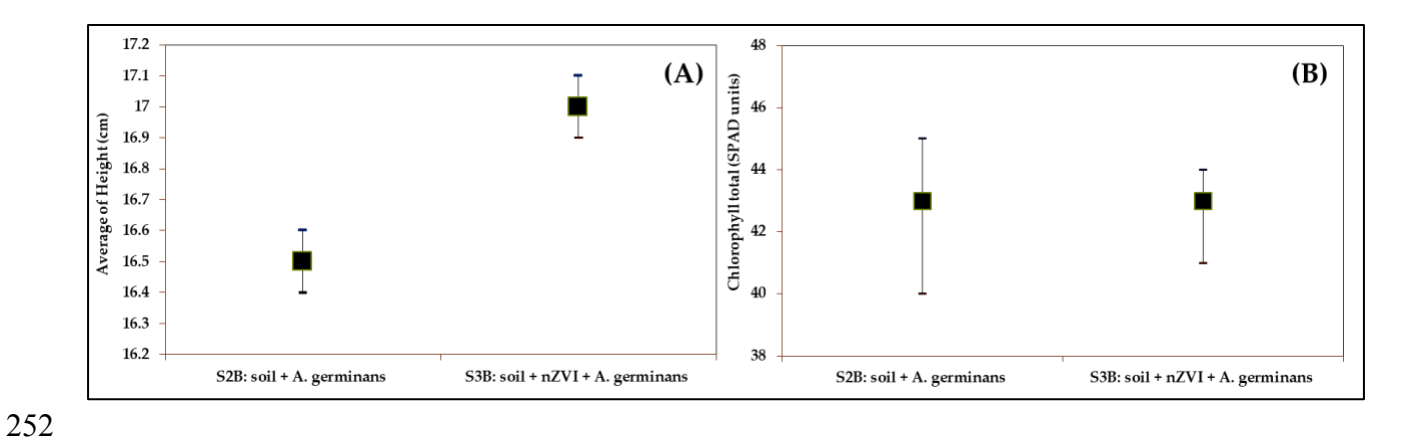


Figure 5. Variation of Chlorophyll content (SPAD units) and measures of height (cm) of *A. germinans* in control (S2B) and treated (S3B) systems with 3g/L of nZVI during an exposure period of 5 months (S3B). Means \pm SD (n=20). Graph (**A**) show the range of average height and graph (**B**) show the chlorophyll total obtained of S2B and S3B systems, respectively.

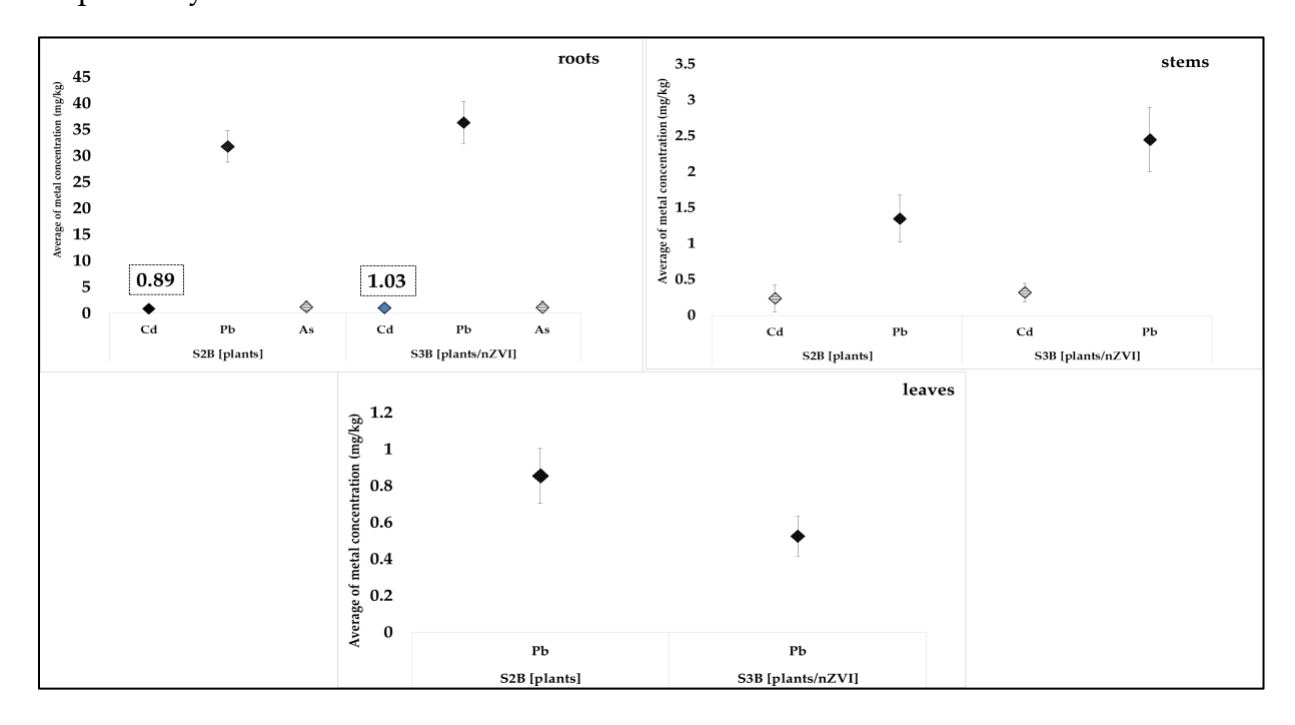


Figure 6. Average (mg/kg) of As, Cd, and Pb concentrations in roots, stems, and leaves tissues of *A. germinans* in control and treated systems (n=20). Rectangle shows the average Cd concentration for each system.

Figure 6 shows the mobility of Cd, Pb, and As metals in the different tissues of *A. germinans* in the systems S2B and S3B. The metal with highest concentration in the roots

is Pb followed by Cd and As. In system S3B, the concentration of Cd in the roots is higher than in system S2B, which reflects that the nZVI facilitate the entrance of this metal into the roots of *A. germinans*. We propose that the increase in heavy metals in the roots using nZVI can be attributed to the retention of the iron NPs in the apoplast or in the outer layers of the roots (Martínez-Fernández and Komárek, 2016).

In natural conditions, studies suggest that the radical architecture present in *A. germinans* plants might alter the uptake of Cd through an integrated network of multiple response processes such as production of organic acids, antioxidative response, cell wall lignification, and suberization (González-Mendoza et al., 2013). The high average concentrations of Pb in the stem was found in the system S3B, followed by Cd ions, see Fig. 6. For both metals, the system S3B resulted with the highest average concentration translocated from roots to the stems. This confirmed our hypothesis that this treatment reduced the concentration of both metals in the system due to the interaction of nZVI with the plants and facile mobility of these nZVI. As values obtained were below to the detection limit for ICP-AES (0.002 ppm); the metal is integrated into the roots, but not in other aerial plant tissues. This is probably due to the bioavailable form in which As ions are found. In addition, this may be due to the ability of mangroves to exclude or regulate uptake of metals at root level and limit translocation to the shoot (MacFarlane and Burchett, 2002).

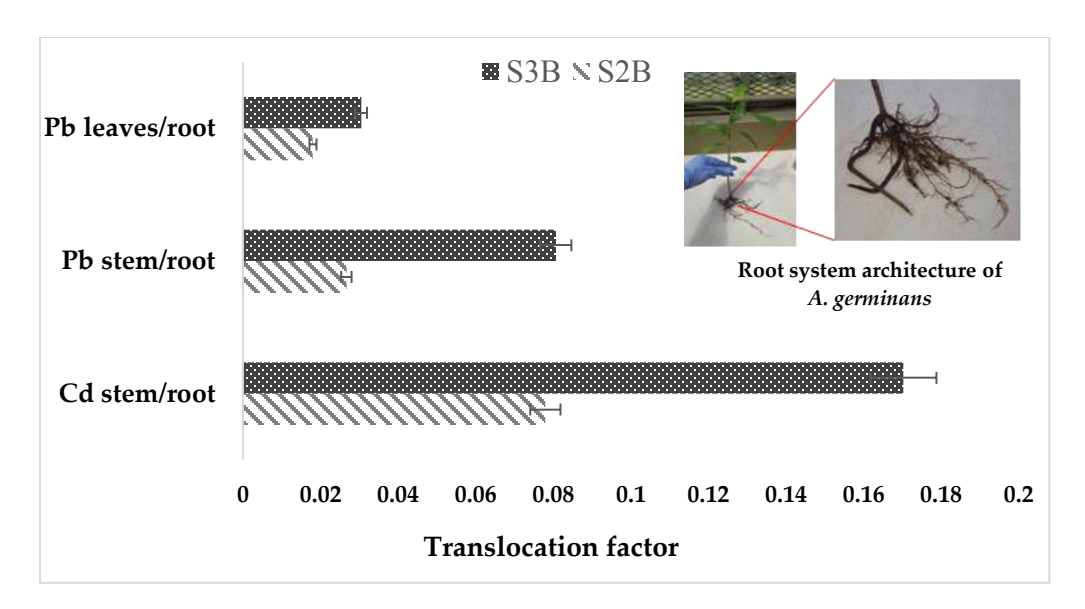


Figure 7. Translocation factor of Pb and Cd in A. germinans in control and treated systems: Pb-leaves/root, Pb-stem/root, and Cd-stem-root.

282

283

284

285

286

287

294

295

296

281

Results for Pb concentrations analysis, in both systems, showed the introduction of this metal into the roots and further translocation into the leaves. S3B presented the highest Pb average concentration in the leaves. These results are confirmed by XPS analysis, in which the presences of iron oxides were detected in both the stem and leaves of A. germinans samples.

Figure 7 compares the translocation factor for each metal as it migrates through the different plant tissues. These results suggested that the system S3B is the most efficient in transporting Pb and Cd ions from roots to stem, and finally to leaves, in case of Pb. This data supports the interpretation that the interaction of nZVI with *A. germinans* facilitates the mobility of these metals to the leaves, where they can be more easily expulsed, most likely through a mechanism of decontamination. These results compare with several studies that have suggested that many plants retain Pb²⁺ in their roots via absorption and precipitation with only minimal transport to the aboveground harvestable plant portions (Tangahu et al., 2011).

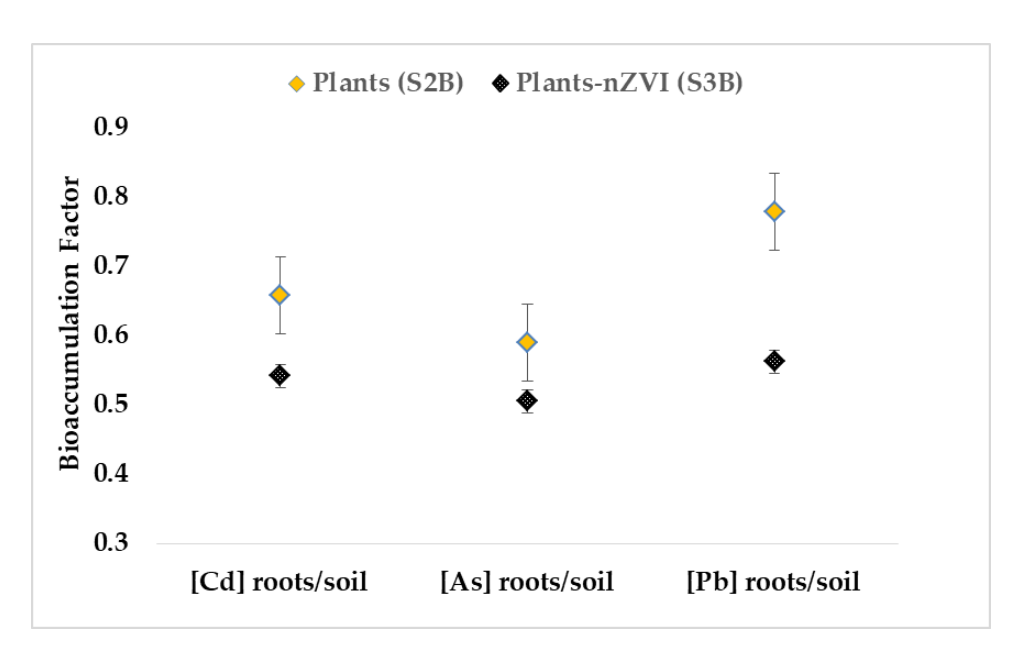


Figure 8. Bioaccumulation factor of Cd, As and Pb concentrations in *A. germinans* control and treated soil systems. The dashed circles group the differences between treatment S2B and S3B for each metal. The largest difference in BAF between S2B and S3B was for Pb.

In Figure 8, the bioaccumulation factors are displayed for Cd, As, and Pb ions in S2B and S3B. S2B showed the highest values for BAF indicating that *A. germinans* bioaccumulate these metals in their tissues, primarily in the roots.(MacFarlane and Burchett, 2002) It has been found that metals such as Cu, Zn, Pb, Fe, Mn, and Cd tend to accumulate primarily in root tissue, rather than in foliage, in mangrove species such as *Avicennia spp.*(Peters et al., 1997)

A BAF < 1 combined with a TF < 1 for both S2B and S3B systems, indicates that A. germinans is not working as a hyperaccumulator plant, but rather as excluders for Cd and Pb metals.

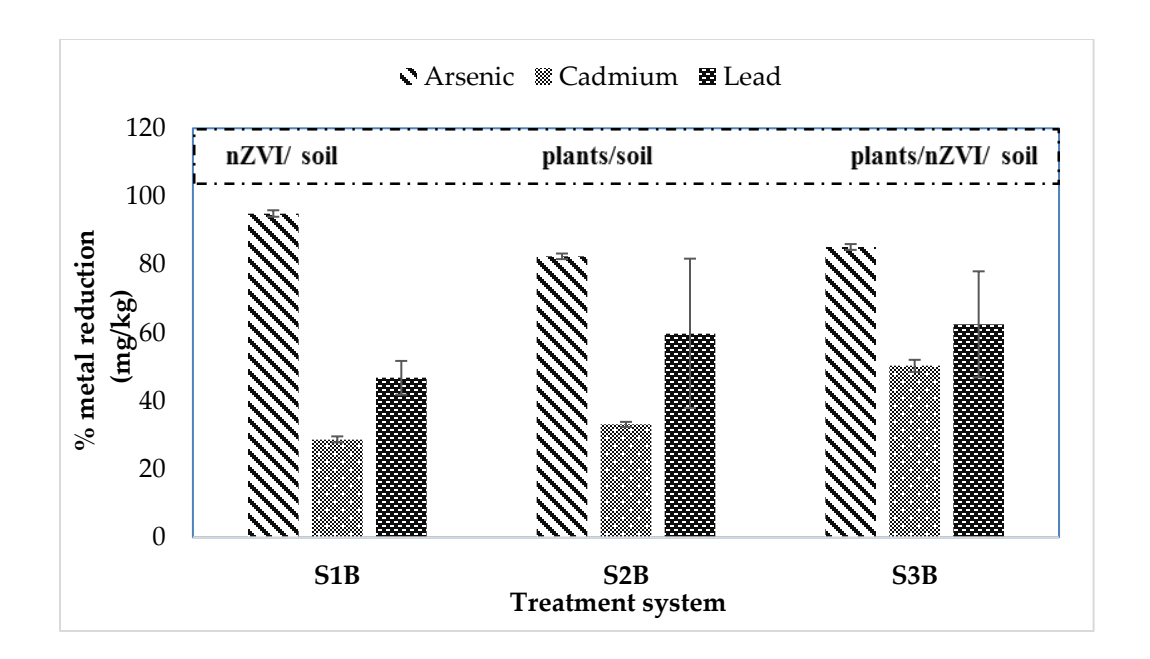


Figure 9. Percentage of As, Cd and Pb metals reduction in treated soil systems.

Figure 9 present the percentage of metal reduction in each system. The highest removal efficiency percent of As by any system was observed in S1B; the nZVI particles present reduced the concentration by 95%. The other systems showed significant As concentration reductions as well: an 82.44% reduction in S2B and an 85.19% reduction in S3B. Cd concentrations were reduced in S1B by 28.74%, in S2B by 33.13% and in S3B by 50.30%. The Pb concentrations showed a similar incremental trend, with S1B at 46.81%, S2B at 59.84% and S3B at 62.49% reduction.

All three systems are shown to efficiently reduce the concentration of As, Cd, and Pb present in the wetland soil. The system that showed the highest reduction in concentration of As was S1B, followed by S3B, and finally S2B. This demonstrates that nZVI are an efficient nanomaterial for the removal of As soil contaminants; furthermore, these results also indicate that the interaction of nZVI with *A. germinans* enhances the permeability of the metal into the plant, as seen in the increased reduction of S3B. Considering Cd and Pb concentrations, the most efficient systems in decreasing order were S3B > S2B > S1B. In this case as well, the interaction of these plants and nZVI helped

to move the cadmium and lead ions more rapidly into the tissue system.

Redox conditions of soil and sediment determine the heavy metals mobility. The Pourbaix diagram for iron demonstrates the stability of hematite (Fe₂O₃) under oxidizing conditions at the pH range of the soil (approximately 6 to 8) (Barnum, 1982; Beverskog and Puigdomenech, 1996; Delahay et al., 1950; Pesterfield et al., 2012). However, due to the complex conditions of the soil, the nZVI can oxidize into other less common iron oxide species (Fe(OH)3 or FeOOH). In this case, the pH values in the organic matter at Cienaga las Cucharillas were in the range of 6 to 8. This may be attributed to chemical feasibility of the fixation of As to the oxidized iron nanoparticle (Fe₂O₃) surfaces. This fixation of As to iron oxide is an important reaction in the subsurface soil because arsenate (AsO₄³⁻) adsorbs strongly to iron oxide surfaces in acidic and near-neutral pH conditions. Iron oxide occurs at approximately pH 8, where As (III) and As (V) are adsorbed to both positively and negatively charged surfaces; as the pH increases in the system, As (V) is desorbed from Fe(OH)₃, and this rate of desorption can be quite high. It is important to identify the pH of the soil to understand the interaction of nZVI with the metals present, especially when iron is oxidized so that it can be more effective in absorbing arsenic on their surface.

345

346

347

348

349

350

351

352

353

354

328

329

330

331

332

333

334

335

336

337

338

339

340

341

342

343

344

Physicochemical analysis in collected water of the systems after treatment

The result of physicochemical analysis of water was carried out on the system weekly for a period of 5 months. These results are presented in Table S1. The pH fluctuated between 7.6 and 8.8. In the treated water, the pH measurements met up with World Health Organization standards for drinking water between the ranges of 6.4 to 8.5.

An increase or decrease in temperature may not necessarily mean reduction in level of impurities or heavy metals. Soil ORP values, at pH 7, found in the literature were used to characterize the soil in four classes: oxidized (> +300 mV), moderately reduced (+100 to +300 mV), reduced (-100 to +100 mV), or highly reduced (< -100 mV).

Conductivity results show similar values for all the systems, because the direct input of metals is not the same as when they are introduced in natural conditions.

Surface Characterization of A. germinans tissue

The A. germinans samples were characterized by XPS and HRTEM. Figure 10 presents the XPS spectra for (a,b) leaf and (c,d) stem samples. Deconvolution of these spectra show that these nZVI particles are incorporated mainly in the leaves and stem of these plants. Deconvolution of the O 1s binding energy region for the leaf sample (Fig. 10 left) results in four peaks at 529.9, 531.8, 533.0, and 534.7 eV. These peaks correspond to a metal oxide species (Fe₂O₃), metal hydroxide species (Fe(OH)_x), coordinated water to an ionic metal (Fe(H₂O)_x), and water respectively.

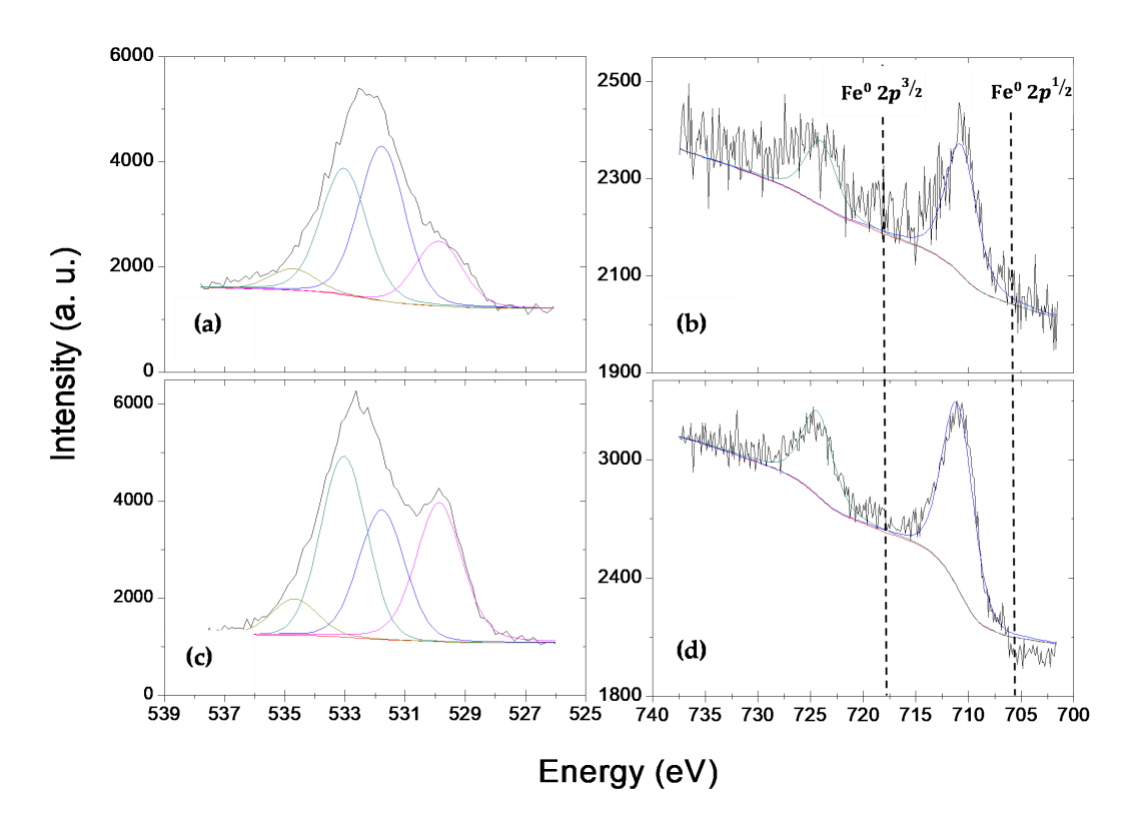


Figure 10. X-ray photoelectron spectroscopy for (a,b) leaf and (c,d) stem samples. The O1s binding energy region deconvolutions (left) for both samples show the binding energies

for: metal oxide species (Fe₂O₃) (pale red), metal hydroxide species (Fe(OH)_x) (blue), coordinated water to an ionic metal (Fe(H₂O)_x) (green), and water (black). (right) The Fe 2p binding energy region.

Deconvolution of these spectra show that these nZVI particles are incorporated mainly in the leaves and stem of these plants. Deconvolution of the O 1s binding energy region for the leaf sample (Fig. 10 left) results in four peaks at 529.9, 531.8, 533.0, and 534.7 eV. These peaks correspond to a metal oxide species (Fe₂O₃), metal hydroxide species (Fe(OH)_x), coordinated water to an ionic metal (Fe(H₂O)_x), and water respectively.

Iron is only present in its oxidized form, illustrated in the deconvolution of the Fe 2p region, where the only peaks present are at 710.7 and 724 eV. There is no signal for Fe⁰ (706 and 719 eV). Continuing to the stem sample, the deconvolution of the O 1s region is similar generating four peaks, as well: 529.9, 531.8, 533.0, and 534.6 eV; however, the relative intensities of these peaks are different. The cross section for different plant regions is diverse which might suggest why the relative intensities are different.

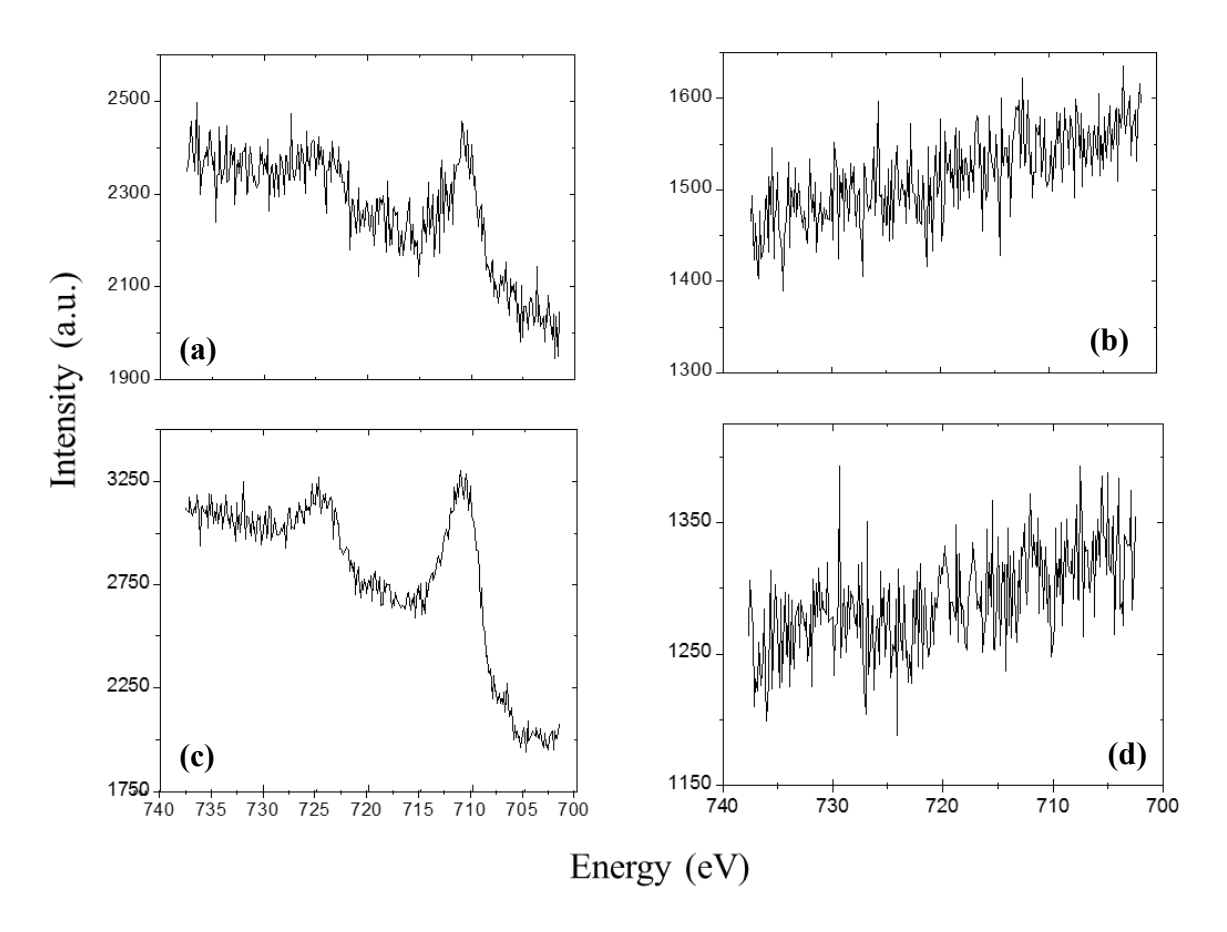


Figure 11. Comparisons of the Fe 2p binding energy region for leaf samples (a) with nZVI and (b) without nZVI, stem samples (c) with nZVI and (d) without nZVI.

A comparison of the Fe 2p region for leaves and stem of *A. germinans* (control and treated samples) in system S2B and S3B is shown in Fig. 11. The Fe₂O₃ and Fe(H₂O)_x peaks are much more pronounced in the stem than in the leaves. Furthermore, the Fe 2p region peaks coincide with those of the leaf (711.0 and 724.4 eV) but have much less background noise and higher counts. By contrast, the Fe 2p region of the root sample contains no Fe peaks. Side by side comparisons of samples from plants treated and untreated with nZVIs show evidence that the resulting Fe signals may be due to the presence of these nanoparticles within the plant matrix. These results confirm that these nZVI particles migrate through the plant and are finally retained in its leaves. The absence of metallic Fe only indicates that these nanoparticles are fully oxidized on their surface; since XPS is

highly surface sensitive, it is possible that they might possess a small metallic core which is beyond the detection range of this technique. In our previous work(Soto Hidalgo et al., 2016) on nZVI, where bulk sensitive techniques, such as X-ray absorption spectroscopy (XAS), were used instead of XPS, suggests that there is indeed a metallic core when you do the linear combination curve fitting.

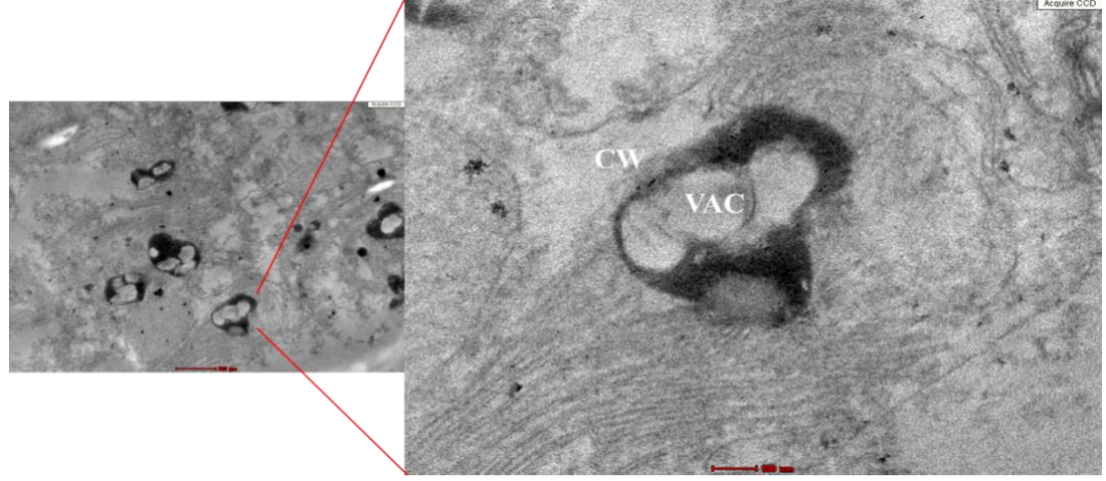


Figure 12. TEM images of vacuoles from *A. germinans* leaves with nZVI treatment in the system S3B (CW = cell wall, VAC = vacuole). Scale: 100nm.

Complimentary to the XPS results, HRTEM images were taken of nZVI treated *A. germinans* (see Fig. 12). The darker areas observed in these images can be ascribed to nanoparticles located inside the vacuoles. The existence of iron NPs in the shoots' tissue intercellular space suggest that NPs are able to pass through the epidermis and cortex via apoplastic pathways, and their small particle size allows for mobility through the transmembrane pathway (Wang et al., 2016).

Conclusions

The analysis of metal concentrations in seeds and tissues of *A. germinans* showed the mobility of Pb and Cd metals. Results obtained in this study suggested that Pb ions have the highest average concentration of all studied contaminants in all analysis done, probably due to their chemical speciation. The availability and mobility of metal ions increased due to the chemical form in which these metal ions are present in the environment. The constructed phytonanoremediation system was an efficient instrument to evaluate the interaction of *A. germinans* and nZVI, combined and separate, for the remediation of Cd, As and Pb in soil and water.

The S1B, S2B, and S3B systems demonstrated high reductions in concentration of As, Cd, and Pb metals. The highest reduction percentage of Cd and Pb concentration was obtained in the S3B system, which means that *A. germinans* in contact with nZVI for a period of 5 months of interaction was the most efficient in removing these heavy metals. This confirms our hypothesis that this interaction promotes the decontamination process via the *A. germinans* without affecting the plant's physiology. The S3B (plants/nZVI) treatment demonstrated be is an excellent alternative to reduce high concentrations of these heavy metals from soil contaminated in wetland. ICP-AES analysis was done for *A. germinans* in system S2B and S3B. These results indicated that the S3B system showed greater mobility for Pb and Cd species to aerial parts of the plants, which means that the presence of nZVI in *A. germinans* facilitates the entrance of the ions.

The presence of Arsenic ions was found into the roots, but not in other aerial plant tissues. This is probably due to the bioavailable form in which the As ions are present in the soil. Experimental values for BAF < 1 and TF < 1 for S2B and S3B systems indicate that *A. germinans* is not working as a hyperaccumulator plant, but rather as an excluder for Cd and Pb metals. XPS analysis for *A. germinans* in systems S2B and S3B confirmed the presence of Fe oxides in the stems and leaves of the plants in S3B. These results confirm that these nZVI particles migrate through the plant and are finally retained in its leaves. The significant increase in iron concentration in the plant tissues indicates that the iron from nZVI was bioavailable as well.

The data obtained in this study suggests that the interaction of nZVI with A. germinans is a novel and efficient way to enhance the bioavailability of Pb²⁺ and Cd²⁺ and help to mangroves to better translocate these contaminants into the stems and leaves.

Acknowledgements

This project was financially supported by NSF-CREST Center for Innovation, Research and Education in Environmental Nanotechnology (CIRE2N) Grant Number NSF-HRD-1736093. This work made use of the Cornell Center for Materials Research (CCMR) Shared Facilities, which are supported through the NSF MRSEC program (DMR-1719875). The assistance of John Grazul (CCMR) is greatly appreciated. KTRH acknowledge the financial support of Puma Energy (Puerto Rico).

Supporting Information Available. The following file is available free of charge. Supporting Information Phytonanoremediation. The supporting information material

- 462 presents Cienaga Las Cucharillas Location, Sampling and Characterization of
- 463 Contaminated Wetland Soil, Physicochemical Water Analysis and Nanoremediation
- 464 System Water Analysis.

466 References

- Bae, S., Collins, R.N., Waite, T.D., Hanna, K., 2018. Advances in Surface Passivation of
- 468 Nanoscale Zerovalent Iron: A Critical Review. Environ. Sci. Technol. 52, 12010-12025.
- Barnum, D.W., 1982. Potential-pH diagrams. J. Chem. Educ. 59, 809.
- 470 Beverskog, B., Puigdomenech, I., 1996. Revised pourbaix diagrams for iron at 25–300 °C.
- 471 Corros. Sci. 38, 2121-2135.
- 472 Bolade, O.P., Williams, A.B., Benson, N.U., 2020. Green synthesis of iron-based
- 473 nanomaterials for environmental remediation: A review. Environ. Nanotechnol. Monit.
- 474 Manag. 13, 100279.
- Dahmani-Muller, H., van Oort, F., Gélie, B., Balabane, M., 2000. Strategies of heavy metal
- 476 uptake by three plant species growing near a metal smelter. Environ. Pollut. 109, 231-238.
- Delahay, P., Pourbaix, M., Van Rysselberghe, P., 1950. Potential-pH diagrams. J. Chem.
- 478 Educ. 27, 683.
- 479 Dong, H., Li, L., Lu, Y., Cheng, Y., Wang, Y., Ning, Q., Wang, B., Zhang, L., Zeng, G.,
- 480 2019. Integration of nanoscale zero-valent iron and functional anaerobic bacteria for
- 481 groundwater remediation: A review. Environ. Int. 124, 265-277.
- 482 Garg, S., Jiang, C., Waite, T.D., 2018. Impact of pH on Iron Redox Transformations in
- 483 Simulated Freshwaters Containing Natural Organic Matter. Environ. Sci. Technol. 52,
- 484 13184-13194.
- 485 González-Mendoza, D., Espadas y Gil, F., Escoboza-García, F., Santamaría, J.M., Zapata-
- 486 Pérez, O., 2013. Copper Stress on Photosynthesis of Black Mangle (Avicennia germinans).
- 487 An. da Acad. Bras. Ciênc. 85, 665-670.
- 488 Hall, J.L., 2002. Cellular mechanisms for heavy metal detoxification and tolerance. J. Exp.
- 489 Bot. 53, 1-11.
- 490 Kamnev, A.A., van der Lelie, D., 2000. Chemical and Biological Parameters as Tools to
- 491 Evaluate and Improve Heavy Metal Phytoremediation. Bioscience Reports 20 (4).
- 492 Kim, C., Ahn, J.-Y., Kim, T.Y., Shin, W.S., Hwang, I., 2018. Activation of Persulfate by
- 493 Nanosized Zero-Valent Iron (NZVI): Mechanisms and Transformation Products of NZVI.
- 494 Environ. Sci. Technol. 52, 3625-3633.
- 495 Kocur, C.M., Chowdhury, A.I., Sakulchaicharoen, N., Boparai, H.K., Weber, K.P.,
- 496 Sharma, P., Krol, M.M., Austrins, L., Peace, C., Sleep, B.E., O'Carroll, D.M., 2014.
- 497 Characterization of nZVI Mobility in a Field Scale Test. Environ. Sci. Technol. 48, 2862-
- 498 2869.

- 499 Liphadzi, M.S., Kirkham, M.B., 2006. Heavy-metal displacement in chelate-treated soil
- with sludge during phytoremediation. J. Plant Nutr. Soil Sci. 169, 737-744.
- MacFarlane, G.R., Burchett, M.D., 2002. Toxicity, growth and accumulation relationships
- of copper, lead and zinc in the grey mangrove Avicennia marina (Forsk.) Vierh. Mar.
- 503 Environ. Res. 54, 65-84.
- Martínez-Fernández, D., Komárek, M., 2016. Comparative effects of nanoscale zero-
- valent iron (nZVI) and Fe₂O₃ nanoparticles on root hydraulic conductivity of Solanum
- 506 lycopersicum L. Environ. Exp. Bot. 131, 128-136.
- 507 Paz-Alberto, A.M., Sigua, G.C., 2013. Phytoremediation: A Green Technology to Remove
- 508 Environmental Pollutants. Am. J. Clim. Change 2, 16.
- 509 Percival, G., P. Keary, I., Noviss, K., 2008. The Potential of a Chlorophyll Content SPAD
- Meter to Quantify Nutrient Stress in Foliar Tissue of Sycamore (Acer pseudoplatanus),
- 511 English Oak (Quercus robur), and European Beech (Fagus sylvatica). Vol 34.
- Pesterfield, L.L., Maddox, J.B., Crocker, M.S., Schweitzer, G.K., 2012. Pourbaix (E–pH-M)
- 513 Diagrams in Three Dimensions. J. Chem. Educ. 89, 891-899.
- 514 Peters, E.C., Gassman, N.J., Firman, J.C., Richmond, R.H., Power, E.A., 1997.
- 515 Ecotoxicology of tropical marine ecosystems. Environ. Toxicol. Chem. 16, 12-40.
- 516 Plekhanov, S.E., Chemeris, Y.K., 2003. Early Toxic Effects of Zinc, Cobalt, and Cadmium
- on Photosynthetic Activity of the Green AlgaChlorella pyrenoidosaChick S-39. Bio. Bull.
- 518 Russ. Acad. Sci. 30, 506-511.
- Raskin, I., Ensley, B.D., 2000. Phytoremediation of toxic metals: using plants to clean up
- 520 the environment, in: Ensley, B.D. (Ed.), Why Use Phytoremediation? . John Wiley, New
- 521 York:, pp. 3-12.
- 522 Soto-Hidalgo, K.T., Ortiz-Quiles, E.O., Betancourt, L.E., Larios, E., José-Yacaman, M.,
- 523 Cabrera, C.R., 2016. Photoelectrochemical Solar Cells Prepared From Nanoscale
- Zerovalent Iron Used for Aqueous Cd²⁺ Removal. ACS Sustain. Chem. Eng. 4, 738-745.
- Tangahu, B.V., Sheikh Abdullah, S.R., Basri, H., Idris, M., Anuar, N., Mukhlisin, M., 2011.
- 526 A Review on Heavy Metals (As, Pb, and Hg) Uptake by Plants through
- 527 Phytoremediation. Int. J. Chem. Eng. 2011, 31.
- Wang, J., Fang, Z., Cheng, W., Yan, X., Tsang, P.E., Zhao, D., 2016. Higher concentrations
- of nanoscale zero-valent iron (nZVI) in soil induced rice chlorosis due to inhibited active
- iron transportation. Environ. Pollut. 210, 338-345.
- Zhang, W., Ebbs, S.D., Musante, C., White, J.C., Gao, C., Ma, X., 2015. Uptake and
- 532 Accumulation of Bulk and Nanosized Cerium Oxide Particles and Ionic Cerium by
- Radish (Raphanus sativus L.). J. Agric. Food Chem. 63, 382-390.
- 534 Zou, Y., Wang, X., Khan, A., Wang, P., Liu, Y., Alsaedi, A., Hayat, T., Wang, X., 2016.
- 535 Environmental Remediation and Application of Nanoscale Zero-Valent Iron and Its
- 536 Composites for the Removal of Heavy Metal Ions: A Review. Environ. Sci. Technol. 50,
- 537 7290-7304.

- 538 Soto Hidalgo, K. T.; Guzman-Blas, R.; Ortiz-Quiles, E. O.; Fachini, E. R.; Corchado-
- García, J.; Larios, E.; Zayas, B.; Jose-Yacaman, M.; Cabrera, C. R. Highly Organized
- 540 Nanofiber Formation from Zero Valent Iron Nanoparticles after Cadmium Water
- 541 Remediation. RSC Adv. 2015, 5, 2777–2784.).
- 542 Azzazy M. F. (2020). Plant bioindicators of pollution in Sadat City, Western Nile Delta,
- 543 Egypt. *PloS one*, 15(3), e0226315. https://doi.org/10.1371/journal.pone.0226315
- Blande, J. D., Holopainen, J. K., & Niinemets, U. (2014). Plant volatiles in polluted
- atmospheres: stress responses and signal degradation. Plant, cell & environment, 37(8),
- 546 1892–1904. https://doi.org/10.1111/pce.12352